Syntheses and Solid-state Structures† of Trimeric Dibenzylamidolithium and its Diethyl Ether and Hexamethylphosphoramide Dimeric Complexes: an Explanation of these Structures and Evidence for Li • • • CH Interactions in both Solid and Solution Phases

David R. Armstrong, Robert E. Mulvey, and Gordon T. Walker
Department of Pure and Applied Chemistry, University of Strathclyde, 295 Cathedral Street, Glasgow G1 1XL
Donald Barr and Ronald Snaith *
University Chemical Laboratory, Lensfield Road, Cambridge CB2 1EW
William Clegg
Department of Inorganic Chemistry, The University, Newcastle upon Tyne NE1 7RU
David Reed
Department of Chemistry, University of Edinburgh, West Mains Road, Edinburgh EH9 3JJ

Dibenzylamidolithium, $[(PhCH_2)_2NLi]_n$, (**1**), and two of its complexes, $[(PhCH_2)_2NLi{\cdot}OEt_2]_n$, (**2**), and $[(PhCH_2)_2NLi{\cdot}hmpa]_n$, (**3**) (hmpa = hexamethylphosphoramide), have been synthesised and characterised, and shown to meet earlier proposed criteria for useful proton abstraction reagents. The *X*-ray crystal structures of (**1**), (**2**), and (**3**) have been determined. Their solid-state structures contain central $(NLi)_n$ rings [n = 3 for (**1**), n = 2 for (**2**) and (**3**)], and the diminution in ring size from six- to four-membered on complexation of (**1**) has been rationalised *via* the results from *ab initio* calculations on model systems. Recent ring-stacking and ring-laddering principles have also been used to show why such rings cannot associate further, so leaving their lithium atoms with abnormally low co-ordination numbers [formally only 2 in (**1**), 3 in (**2**) and (**3**)]. Evidence that the co-ordinatively unsaturated Li atoms, in (**1**) in particular, are thereby prompted to engage in compensating interactions with CH units on the $(PhCH_2)_2N$ ligands is drawn from both solid-state and solution studies. For the former, the implications of relatively short Li • • • HC distances in the structure of (**1**) have been probed by molecular orbital bond index (MOBI) calculations which show that Li • • • HC interactions constitute *ca.* 40% of lithium's valency, and that C–H bonds involved are weakened. In the solution studies, cryoscopic, ^{7}Li n.m.r. spectroscopic, and u.v.–visible spectroscopic measurements have shown that the pink-red solution colours of (**1**) and (**2**) are caused by a species common to both, monomeric $(PhCH_2)_2NLi$; m.o. calculations on this one-co-ordinate Li species imply that it contains enhanced Li • • • benzyl interactions which shift the charge transfer transition h.o.m.o. (benzyl) ⟶ l.u.m.o. (Li) (highest occupied and lowest unoccupied molecular orbitals, respectively) into the visible region.

Amidolithium compounds, $(RR'NLi)_n$, and their complexes with Lewis bases L, $(RR'NLi{\cdot}L)_n$, have been extensively used both to prepare amides of other metals[1] and selectively to abstract protons in organic syntheses where the substrate is susceptible to competitive nucleophilic addition.[2] With notable exceptions, such as $[(Me_3Si)_2NLi]_n$[2b,3] and $[(Me_3Si)_2NLi{\cdot}OEt_2]_n$,[4] such reagents have normally been prepared then used *in situ*, without prior isolation. As part of our studies on these species we reported recently[5] on the family comprising dibenzylamidolithium, $[(PhCH_2)_2NLi]_n$, (**1**), and its diethyl ether and hexamethylphosphoramide complexes, $[(PhCH_2)_2NLi{\cdot}OEt_2]_n$, (**2**), and $[(PhCH_2)_2NLi{\cdot}hmpa]_n$, (**3**) [hmpa = $OP(NMe_2)_3$, hexamethylphosphoramide], respectively. Here we elaborate on the aforesaid preliminary communication and include subsequent results, concentrating on the following aspects. (*i*) The syntheses and characterisations of (**1**), (**2**), and (**3**), and their possible advantages as proton abstraction reagents. (*ii*) Their solid-state structures as determined by *X*-ray crystallography. First, aided by results from *ab initio* molecular orbital (m.o.) calculations, we rationalise why complexation causes a diminution of observed $(NLi)_n$ ring size from n = 3 in (**1**) to n = 2 in complexes (**2**) and (**3**). Secondly, using recently developed ring-stacking[6] and ring-laddering[7] principles, we show how the stereochemistry of the $(PhCH_2)_2N$ groups prevents these rings from associating further, either vertically or laterally. (*iii*) From such considerations, we argue that the resulting low-co-ordinate Li atoms within such rings [particularly in (**1**) where Li is merely two-co-ordinate] engage in compensatory intramolecular interactions with CH units on the amide groups; evidence for such interactions, both in the solid state and in solution, is drawn from *X*-ray crystallographic, m.o. calculational, and cryoscopic data, and from u.v.–visible and n.m.r. spectroscopic measurements.

Results and Discussion

Preparation, Characterisation, and likely Synthetic Uses of the Amidolithium Compounds.—Addition of equimolar amounts of n-butyl-lithium in hexane to chilled solutions of dibenzylamine in toluene–hexane for (**1**), diethyl ether–hexane for (**2**), and hmpa–hexane for (**3**) immediately produced very pale pink, or red [for (**3**)], solids in more deeply coloured solutions. Warming, with addition of further toluene in the case of (**1**), effected complete dissolution. Cooling of the solutions for *ca.* 1 h at −10 °C then gave the crystalline products. Details of yields, physical properties of the products, and analytical data are given in Table 1. Of especial interest, the lability of diethyl ether

† *Supplementary data available:* see Instructions for Authors, *J. Chem. Soc., Dalton Trans.*, 1988, Issue 1, pp. xvii—xx.

Non-S.I. unit employed: cal = 4.184 J.

Table 1. Physical and analytical data for the dibenzylamidolithium compounds

Compound	Description	Yield (%)	M.p. (°C)	Analysis (%)[a] C	H	Li	N	P
(1)	Thin pale pink plates	85	146—148	82.8 (82.6)	6.9 (7.4)	3.5 (3.3)	6.9 (7.1)	
(2)	Thin pale pink plates	80	146—148[b]	78.0 (77.3)	8.7 (8.8)	2.5 (2.8)	5.1 (5.2)	
(3)	Large red-purple blocks	70	110—112	62.8 (62.0)	8.4 (8.3)	1.8 (1.8)	14.7 (14.0)	8.1 (8.2)

[a] Calculated values in parentheses. [b] The crystals darken and lose diethyl ether at *ca.* 135 °C.

Table 2. Comparative key dimensions for the dibenzylamidolithium compounds*

Compound	Mean ring bond lengths (Å) Li–N	Li···Li	Mean ring bond angles (°) NLiN	LiNLi	Li–donor distances Li–O (Å)
(1)	1.953 (1.907—2.038)	2.885 (2.872—2.909)	143.8 (141.3—147.0)	95.2 (95.0—95.3)	
(2)	1.986 (1.980—1.992)	2.446	104.0	76.0 (75.7—76.3)	2.012
(3)	2.007 (2.001—2.013)	2.505	102.7	77.3	1.850

* Where appropriate, ranges of such dimensions are given in parentheses.

in (2) is indicated by the fact that these crystals first darken before melting at the same temperature as dibenzylamidolithium, (1), itself. The i.r. spectra of these compounds showed that no NH group remained, and that Et_2O and hmpa were present in (2) and (3) respectively; brief air exposure of samples produced spectra indicative of hydrolysis, with ν[Li(O–H)] and ν(N–H) bands at 3 680 and 3 400 cm^{-1} respectively. Similarly, ^1H and ^{13}C n.m.r. spectroscopy confirmed the high purity of the products, the former also substantiating the absence of NH protons and establishing the 1:1 amide:donor stoicheiometry of complexes (2) and (3).

As mentioned in the Introduction, amidolithium species $(RR'NLi)_n$, particularly those with bulky substituents, *e.g.*, lda (lda = lithium di-isopropylamide, R = R′ = Pr^i),[2] lithium tetramethylpiperidide [RR′N = $Me_2C(CH_2)_3CMe_2N$],[2,4a] and bis(trimethylsilyl)amidolithium (R = R′ = Me_3Si),[2,3] are used extensively as selective proton abstractors. Although solutions of lda and $[(Me_3Si)_2NLi]_n$, for example, are commercially available, the usual procedure has been to prepare a solution of the lithium reagent as required, and then to use it forthwith. However, as implied in recent criteria for such reagents,[4a] this procedure has drawbacks: first the need to assume a 100% yield from the amine lithiation (not always a reasonable assumption, *e.g.* when R,R′ groups contain unsaturated functional groups), and secondly the usual need to employ a donor solvent, most $(RR'NLi)_n$ species (*n* representing a high oligomer or polymer) being insoluble in hydrocarbons. Indeed, from this last point, the actual reagent in most cases must be a complex, $(RR'NLi{\cdot}L)_n$. Clearly, therefore, if the selectivity of such reagents is to be understood then their isolation and identification must be a first step, followed by solution studies to pinpoint the actual lithiating species in subsequent reactions, *e.g.* most $(RR'NLi{\cdot}L)_2$ solids, with L a monodentate donor, engage in monomer ⇌ dimer equilibria in arene solutions,[8] and the former will presumably be the more active species.

Compounds (1), (2), and (3) satisfy the above-noted criteria particularly well. They can be made simply and quickly, in high yield (see Table 1), as very pure crystalline materials: typically, 2—4 g batches can be available within *ca.* 2 h. Although air- and moisture-sensitive like most lithium compounds, the crystals are not prohibitively so, and can be weighed out in a glove-box for subsequent reaction. Furthermore, while (1) has rather limited solubility, (2) and (3) are extremely soluble in non-polar solvents (*ca.* 60 and 100 mg cm^{-3} respectively in cold benzene or toluene), and, as recorded later, it has proved possible to identify the precise species present in these solutions and their concentration dependence. Other attributes of these compounds are; (*i*) the cheapness of their precursor dibenzylamine [about one-third the price of $(Me_3Si)_2NH$ for example], and (*ii*) the colours of their solutions. The latter could be a useful aid first to establishing then following subsequent reactions, visually then *via* electronic spectroscopy at variable temperatures [*cf.* solutions of commonly used amidolithium reagents, such as lda and $(Me_3Si)_2NLi$, are colourless or pale yellow]. In summary then, compound (1) and its complexes such as (2) and (3) seem particularly promising amidolithium reagents whose synthetic applications merit investigation.

The Crystal and Molecular Structures of the Amidolithium Compounds.—An *X*-ray crystallographic study has shown that (1) is trimeric in the solid state, containing a central planar six-membered $(NLi)_3$ ring. A view of the molecule from above this ring, incorporating the numbering scheme used, is given in Figure 1, while Figure 2 shows a side-on-view of the molecule (see later discussion). In contrast, the complexes (2) and (3) are dimeric, with planar four-membered $(NLi)_2$ ring systems. Figures 3 and 4 illustrate the structure of (2) in various aspects, and Figure 5 that of (3). Some key comparative bond lengths and angles for all three species are presented in Table 2, and atomic co-ordinates and selected interatomic distances and angles are given respectively in Tables 3—8 for (1), (2), and (3).

Concerning the data in Table 2, numerous solid-state structures are now available for oligomeric amidolithium compounds, $(RR'NLi)_n$, *n* = 4 and 3, and for their 1:1 complexes, $(RR'NLi{\cdot}L)_n$, *n* = 2 and 1, and a general picture is

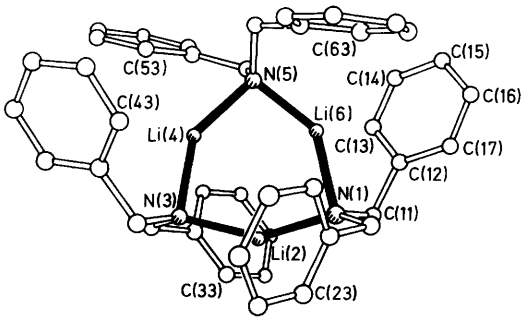

Figure 1. Molecular structure of $[(PhCH_2)_2NLi]_3$, (**1**)

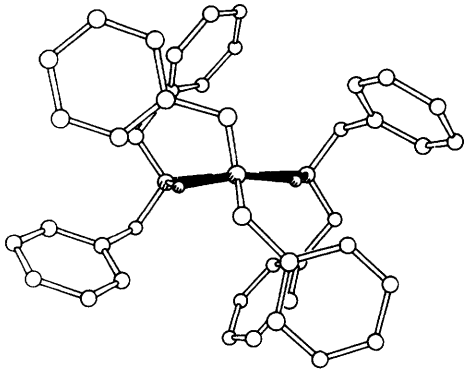

Figure 2. Side-on view of the $(NLi)_3$ ring of (**1**) showing the orientations of benzyl groups relative to this ring

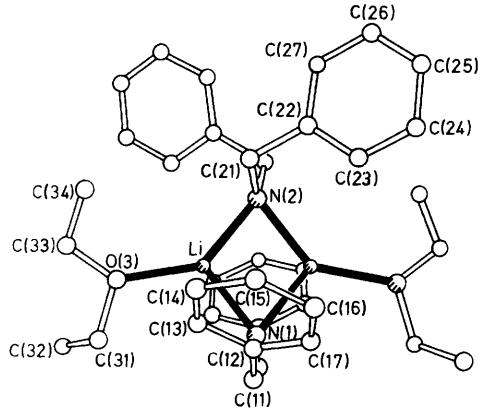

Figure 3. Molecular structure of $[(PhCH_2)_2NLi{\cdot}OEt_2]_2$, (**2**)

emerging of the dimensions to be expected for such species. The Li–N bonds are highly ionic,[9] yet it is possible to infer at least a degree of covalency within them, as their bond lengths show variations intelligible in terms of the co-ordination numbers of their constituent atoms (particularly so for a constant RR'N unit). For example, the mean Li–N bond length in (**1**), whose constituent atoms are formally two- and four-co-ordinate respectively, is 1.953 Å {*cf.* in the only other known trimeric amidolithium, $[(Me_3Si)_2NLi]_3$, 2.005 Å,[3b] and the only known tetramer, $[Me_2C(CH_2)_3CMe_2NLi]_4$, 2.000 Å[4a]}, and so somewhat shorter than those in the dimeric complexes (**2**) (1.986 Å) and (**3**) (2.007 Å), whose Li and N atoms are three- and four-co-ordinate respectively {*cf.* in other dimeric

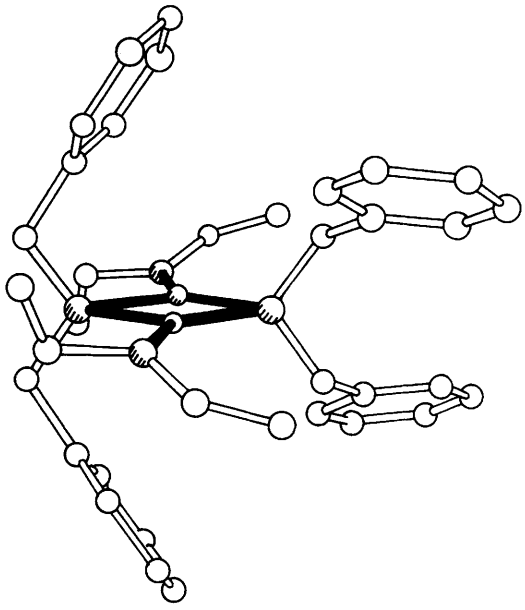

Figure 4. Side-on view of the $(NLi)_2$ ring of (**2**) showing the orientations of benzyl groups and the lateral projections of Et_2O ligands

complexes with similar co-ordination numbers, $[(Me_3Si)_2NLi{\cdot}OEt_2]_2$, 2.055 Å,[4] and $[2,4,6\text{-}Bu^t_3C_6H_2N(H)Li{\cdot}OEt_2]_2$, 2.014 Å[10]}. Metal–nitrogen bonds rather shorter than those in (**1**) can occur in monomeric complexes when both atoms are three-co-ordinate [*e.g.* $2,4,6\text{-}Bu^t_3C_6H_2N(H)Li{\cdot}$tmen, 1.895 Å[11] (tmen = *NNN'N'*-tetramethylethylenediamine)], but bonds even longer than those in (**2**) and (**3**) are found in dimeric complexes where the donor is bidentate, so making both Li and N atoms four-co-ordinate {*e.g.* [Ph(Me)NLi·tmen]$_2$, 2.189 Å[12]}.

The cross-ring Li···Li distances for (**1**) *vs.* (**2**) and (**3**) (column 3 in Table 2) reflect merely the contraction of the ring from six- to four-membered on complexation. In both sizes of ring system, but especially so for the expanded one, a much larger angle is apparent at the metal atom compared to that at the nitrogen atom (columns 4 and 5 of Table 2), and these results are paralleled closely in the angles found at Li and N for the trimer $[(Me_3Si)_2NLi]_3$, 147.6 and 92.3° respectively,[3b] and for its known complexed dimer, $[(Me_3Si)_2NLi{\cdot}OEt_2]_2$, 104.9 and 75.1° respectively.[4] The Li–donor atom distances found in the complexes (**2**) and (**3**) (column 6 of Table 2) also deserve comment as that in the latter, involving hmpa, is exceptionally short: as we have remarked earlier, when reporting the structure of $(Bu^t_2C{=}NLi{\cdot}hmpa)_2$ whose Li–O distance is similar at 1.858 Å, hmpa is clearly a particularly good Lewis base for lithium.[6c,13] A final geometrical point concerns the orientation of the benzyl groups in compound (**1**) and in its complexes (**2**) and (**3**). From Figures 1 and 2, it can be seen that all the phenyl rings of the benzyl units within (**1**) fold back and bend in towards the Li atoms of the $(NLi)_3$ ring: we return to this observation later. In (**2**) and (**3**), just two of the four benzyl units overlap the $(NLi)_2$ rings: for (**2**), as seen from Figures 3 and 4, both are bonded to the same N atom, while for (**3**), shown in Figure 5, it is one unit on each N atom which is so orientated.

Diminution of $(NLi)_n$ *ring size on Lewis base* (L) *complexation.* Complexation of the six-membered $(NLi)_3$ ring of (**1**) causes diminution in ring size to give the $(NLi)_2$ systems of (**2**) and (**3**). This feature occurs elsewhere in organonitrogen–lithium chemistry, as in the conversion of $[(Me_3Si)_2NLi]_3$[3b] to $[(Me_3Si)_2NLi{\cdot}OEt_2]_2$,[4] and of $(Bu^t_2C{=}NLi)_6$ [effectively a stacked pair of trimers, $(Bu^t_2C{=}NLi)_3$[6a,b]] to $(Bu^t_2C{=}NLi{\cdot}$

Table 3. Atomic co-ordinates ($\times 10^4$) for (1)

Atom	*x*	*y*	*z*	Atom	*x*	*y*	*z*
N(1)	7 024(2)	817(2)	2 897(1)	C(41)	9 033(3)	2 815(3)	4 175(2)
C(11)	5 702(3)	602(3)	2 851(2)	C(42)	9 397(3)	3 931(3)	3 652(2)
C(12)	5 272(3)	1 089(2)	1 920(2)	C(43)	10 042(3)	4 046(3)	2 752(2)
C(13)	4 409(3)	2 192(3)	1 720(2)	C(44)	10 318(4)	5 080(4)	2 255(3)
C(14)	4 109(4)	2 691(3)	843(3)	C(45)	9 956(4)	6 012(3)	2 640(3)
C(15)	4 674(5)	2 102(4)	160(3)	C(46)	9 323(4)	5 912(3)	3 529(3)
C(16)	5 512(4)	1 006(4)	354(3)	C(47)	9 046(3)	4 880(3)	4 033(3)
C(17)	5 803(3)	497(3)	1 223(2)	Li(4)	7 501(6)	3 746(5)	2 822(4)
C(21)	8 207(3)	−67(3)	2 589(2)	N(5)	6 903(2)	3 879(2)	1 676(2)
C(22)	9 522(3)	21(2)	2 805(2)	C(51)	5 483(3)	4 602(3)	1 754(2)
C(23)	9 897(3)	−449(3)	3 659(2)	C(52)	5 206(3)	5 742(2)	2 022(2)
C(24)	11 078(3)	−326(3)	3 871(2)	C(53)	6 225(3)	6 135(3)	2 182(2)
C(25)	11 909(3)	285(3)	3 221(3)	C(54)	5 906(4)	7 168(3)	2 454(2)
C(26)	11 560(3)	749(3)	2 361(3)	C(55)	4 556(4)	7 826(3)	2 550(2)
C(27)	10 388(3)	618(3)	2 159(2)	C(56)	3 520(4)	7 449(3)	2 391(3)
Li(2)	7 319(6)	1 468(5)	3 795(4)	C(57)	3 837(3)	6 422(3)	2 130(2)
N(3)	7 668(2)	2 750(2)	4 054(1)	C(61)	7 725(4)	4 319(3)	811(2)
C(31)	6 540(3)	3 339(3)	4 675(2)	C(62)	8 708(3)	3 371(3)	375(2)
C(32)	5 197(3)	3 067(3)	4 663(2)	C(63)	8 173(3)	2 665(3)	74(2)
C(33)	4 983(3)	1 991(3)	5 082(2)	C(64)	9 031(4)	1 796(3)	−328(2)
C(34)	3 801(3)	1 701(3)	5 033(2)	C(65)	10 446(4)	1 621(4)	−442(2)
C(35)	2 823(3)	2 488(3)	4 548(2)	C(66)	10 996(4)	2 305(4)	−172(2)
C(36)	2 997(3)	3 567(3)	4 130(2)	C(67)	10 148(4)	3 173(3)	238(2)
C(37)	4 185(3)	3 849(3)	4 194(2)	Li(6)	7 008(6)	2 258(5)	1 879(4)

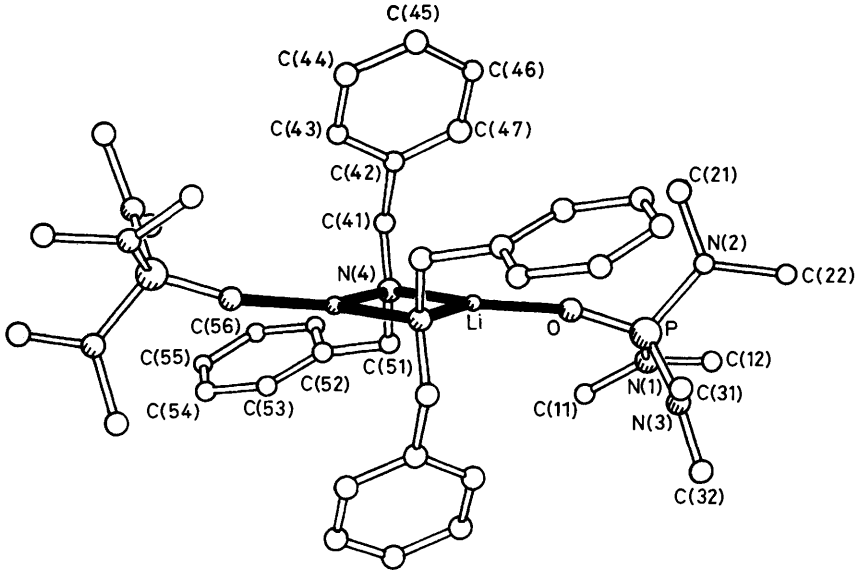

Figure 5. Molecular structure of $[(PhCH_2)_2NLi{\cdot}hmpa]_2$, (3)

hmpa)$_2$,[6c,13] and is explicable qualitatively in terms of the relative merits of the co-ordination sites offered to incoming L molecules by $(NLi)_3$ trimers on the one hand, and by $(NLi)_2$ dimers on the other. Thus, while trimers seem to be the preferred structural unit for uncomplexed species {Figure 6(*a*), for (**1**) and $[(Me_3Si)_2NLi]_3$ [3b]}, within them the angles at Li are large (144—148° in the two amidolithiums just mentioned), so restricting the co-ordination arcs available to incoming donors. In contrast, the angles at Li in an uncomplexed dimer would be much smaller. Significantly, no such $(NLi)_2$ species are known in the solid state, though a guide to the value of such angles is given by that of *ca.* 100° in the gas-phase structure of $[(Me_3Si)_2NLi]_2$:[11] hence such a dimer [Figure 6(*b*)] has a far wider co-ordination arc available for attachment of L molecules.

Although this simple, largely pictorial explanation seems generally adequate, in order to probe this feature more quantitatively, we have carried out *ab initio* geometry optimisations (6-31G basis set) on some model systems. The results for $(H_2NLi{\cdot}H_2O)_n$, where n = 1, 2, and 3, and for $H_2NLi{\cdot}OMe_2$, are shown in Figure 7; those for the latter molecule simply confirm that H_2O is a reasonable mimic for usual oxygen-donating ligands. For all three aqua complexes, the most stable conformation of the water molecule is in a staggered (perpendicular) orientation to the plane of the NH_2 group. Rotation of the water molecules to an eclipsed conformation increases the energy by 1.0, 5.8, and 10.4 kcal mol^{-1} for the monomer, dimer, and trimer respectively. Comparison with the structures of uncomplexed $(H_2NLi)_n$, n =

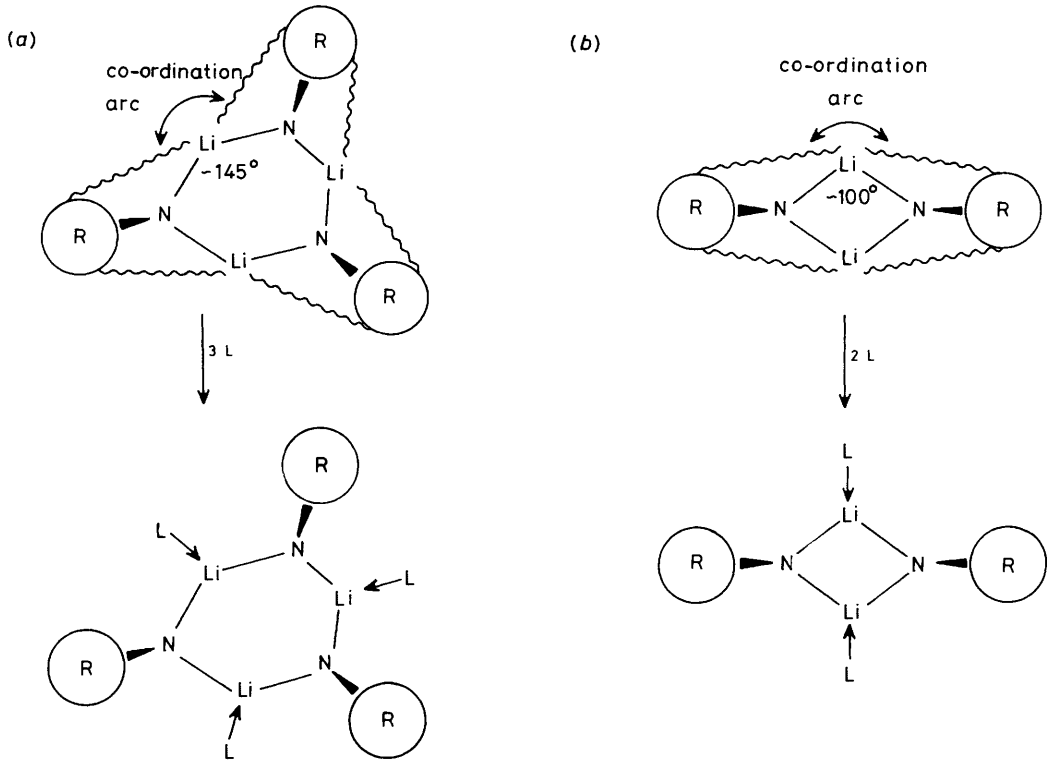

Figure 6. Co-ordination arcs available for formation of amidolithium complexes, $(R_2NLi{\cdot}L)_n$, n = 3 and 2, (*a*) from parent trimers $(R_2NLi)_3$, (*b*) from parent dimers $(R_2NLi)_2$

Table 4. Selected bond lengths (Å) and angles (°) for (**1**)

N(1)–Li(2)	1.907(8)	N(1)–Li(6)	2.038(5)
Li(2)–N(3)	1.907(8)	N(3)–Li(4)	1.979(6)
Li(4)–N(5)	1.951(7)	N(5)–Li(6)	1.938(6)
C(11)–N(1)–C(21)	110.5(3)	C(11)–N(1)–Li(2)	125.7(2)
C(21)–N(1)–Li(2)	115.1(3)	C(11)–N(1)–Li(6)	99.9(2)
C(21)–N(1)–Li(6)	105.5(2)	Li(2)–N(1)–Li(6)	95.0(3)
N(1)–Li(2)–N(3)	147.0(3)	Li(2)–N(3)–C(31)	114.3(3)
Li(2)–N(3)–C(41)	125.4(2)	C(31)–N(3)–C(41)	110.6(3)
Li(2)–N(3)–Li(4)	95.3(3)	C(31)–N(3)–Li(4)	105.5(2)
C(41)–N(3)–Li(4)	101.2(3)	N(3)–Li(4)–N(5)	143.0(4)
Li(4)–N(5)–C(51)	104.7(3)	Li(4)–N(5)–C(61)	119.4(3)
C(51)–N(5)–C(61)	110.1(2)	Li(4)–N(5)–Li(6)	95.2(3)
C(51)–N(5)–Li(6)	113.3(3)	C(61)–N(5)–Li(6)	113.3(3)
N(1)–Li(6)–N(5)	141.3(4)		

Table 5. Atomic co-ordinates ($\times 10^4$) for (**2**)

Atom	*x*	*y*	*z*
Li	4 537(3)	2 487(6)	2 653(5)
N(1)	5 000	1 031(4)	2 500
C(11)	5 310(2)	229(3)	3 378(2)
C(12)	5 661(2)	980(3)	4 327(3)
C(13)	5 355(2)	1 498(4)	4 832(3)
C(14)	5 678(3)	2 225(4)	5 683(3)
C(15)	6 302(2)	2 434(4)	6 037(3)
C(16)	6 612(2)	1 912(5)	5 539(4)
C(17)	6 287(2)	1 199(4)	4 688(3)
N(2)	5 000	3 928(4)	2 500
C(21)	5 267(2)	4 725(3)	3 403(3)
C(22)	5 867(2)	5 388(4)	3 603(2)
C(23)	6 420(2)	4 724(4)	3 894(3)
C(24)	6 978(2)	5 317(5)	4 069(3)
C(25)	6 989(3)	6 561(6)	3 962(3)
C(26)	6 456(2)	7 217(5)	3 680(3)
C(27)	5 901(2)	6 636(4)	3 499(3)
O(3)	3 817(1)	2 158(3)	2 979(2)
C(31)	3 630(2)	872(5)	2 930(3)
C(32)	2 967(2)	628(6)	2 252(4)
C(33)	3 567(3)	2 891(6)	3 498(5)
C(34)	3 853(3)	4 062(6)	3 768(4)

1, 2, or 3,[14] shows that the Li–N bond lengths have increased through (water) co-ordination at Li, with the greatest increase occurring for the trimer. The Li–O co-ordination bond lengths also increase with increased association, and both these trends can be related to more pronounced steric effects at Li as the OLiN angle decreases with increased association. The calculated hydration energies for the monomer, dimer, and trimer, in total −26.4, −38.0, and −40.7 kcal mol^{-1} respectively, also illustrate this point, especially when they are assigned per individual water molecule; *i.e.* −26.4, −19.0, and −13.6 kcal mol^{-1} respectively. The stabilisation energy due to self association is calculated as −58.6 and −95.4 kcal mol^{-1} for the solvated dimer and the solvated trimer respectively. This stabilisation is much weaker than in the unsolvated species where the corresponding values were −73.7 and −133.9 kcal mol^{-1} respectively.[14b]

Insight into the competitive formation of dimers and trimers of the solvated amidolithiums can be obtained by considering the energy of association as a sum of two components. The first term is the calculated energy required to reorganise the monomeric unit, H_2NLi or $H_2NLi{\cdot}H_2O$, into the appropriate

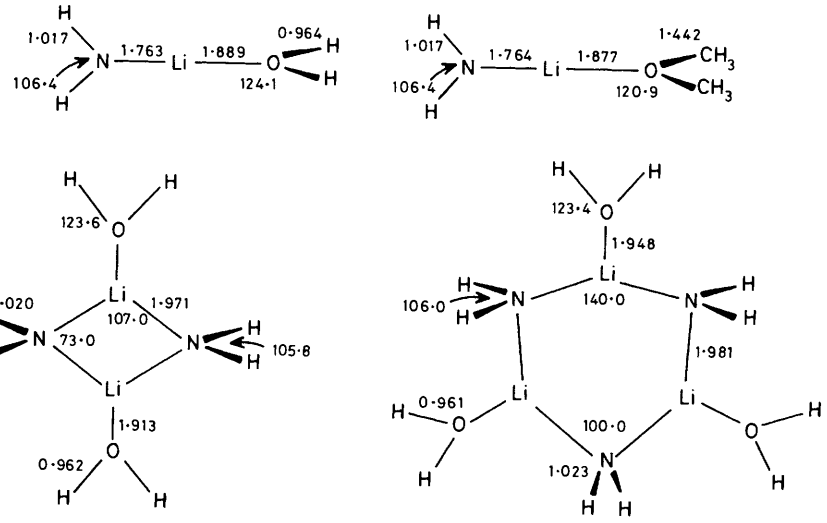

Figure 7. *Ab initio* optimised geometries (6-31G level) of monomeric $H_2NLi{\cdot}H_2O$ and $H_2NLi{\cdot}OMe_2$, and of associated aqua complexes, $(H_2NLi{\cdot}H_2O)_n$, $n = 2$ and 3

Table 6. Selected bond lengths (Å) and angles (°) for (**2**)

Li–N(1)	1.992(8)	Li–N(2)	1.980(8)
Li–O(3)	2.012(9)		
N(1)–Li–N(2)	104.0(4)	N(1)–Li–O(3)	117.6(4)
N(2)–Li–O(3)	138.2(4)	Li–N(1)–C(11)	116.8(3)
Li–N(1)–Li′	75.7(5)	Li–N(1)–C(11′)	119.1(2)
C(11)–N(1)–C(11′)	107.2(4)	Li–N(2)–C(21)	113.0(3)
Li–N(2)–Li′	76.3(5)	Li–N(2)–C(21′)	121.8(2)
C(21)–N(2)–C(21′)	108.6(4)	Li–O(3)–C(31)	115.7(4)
Li–O(3)–C(33)	130.4(4)	C(31)–O(3)–C(33)	111.6(5)

Symmetry operator for primed atoms: $1 - x, y, \frac{1}{2} - z$.

Table 7. Atomic co-ordinates ($\times 10^4$) for (**3**)

Atom	*x*	*y*	*z*
Li	3 996(10)	4 724(4)	4 133(9)
O	2 414(4)	4 327(2)	2 959(4)
P	1 224(2)	3 903(1)	2 303(2)
N(1)	−148(5)	4 211(3)	2 384(6)
C(11)	−32(9)	4 578(5)	3 504(9)
C(12)	−1 584(7)	4 049(5)	1 446(9)
N(2)	910(6)	3 824(3)	774(6)
C(21)	1 280(12)	4 349(6)	122(10)
C(22)	232(12)	3 259(5)	3(10)
N(3)	1 440(6)	3 169(3)	2 887(6)
C(31)	2 682(9)	2 808(4)	2 966(10)
C(32)	626(10)	2 848(4)	3 425(10)
N(4)	4 102(4)	5 623(2)	4 846(4)
C(41)	3 941(7)	6 157(3)	3 992(6)
C(42)	4 748(7)	6 041(3)	3 234(6)
C(43)	6 143(8)	6 185(3)	3 710(7)
C(44)	6 894(8)	6 047(4)	3 010(8)
C(45)	6 259(12)	5 791(5)	1 836(8)
C(46)	4 884(12)	5 662(5)	1 355(9)
C(47)	4 181(8)	5 777(4)	2 058(7)
C(51)	3 162(6)	5 714(3)	5 442(6)
C(52)	3 478(6)	6 273(3)	6 357(6)
C(53)	4 522(8)	6 233(4)	7 553(7)
C(54)	4 834(9)	6 757(4)	8 405(9)
C(55)	4 106(9)	7 306(4)	8 052(10)
C(56)	3 054(10)	7 373(4)	6 866(9)
C(57)	2 761(7)	6 843(3)	6 030(7)

Table 8. Selected bond lengths (Å) and angles (°) for (**3**)

Li–O	1.850(9)	Li–N(4)	2.013(10)
Li–N(4′)	2.001(10)		
O–Li–N(4)	125.6(5)	O–Li–N(4′)	131.2(5)
N(4)–Li–N(4′)	102.7(4)	Li–O–P	165.4(5)
Li–N(4)–C(41)	116.9(5)	Li–N(4)–C(51)	112.6(5)
C(41)–N(4)–C(51)	108.8(5)	Li–N(4)–Li′	77.3(4)
C(41)–N(4)–Li′	118.2(5)	C(51)–N(4)–Li′	120.1(5)

Symmetry operator for primed atoms: $1 - x, 1 - y, 1 - z$.

geometry of the dimer or trimer (*i.e.* lengthening the Li–N bond, and bending the NH_2 unit towards this bond). The second term can be thought of as the energy gained by this reorganised monomeric unit on formation of the extra Li–N bond per unit by association. These energy cycles are presented in Figure 8(*a*) and (*b*) for H_2NLi and $H_2NLi{\cdot}H_2O$ respectively. For the former, the dominant term is the extra stability gained upon association and this is clearly greater for the trimer. The reorganisation energy terms for the dimer and trimer are relatively small. Thus for unsolvated H_2NLi the trimer is the preferred association product. However, examination of the energy terms for $H_2NLi{\cdot}H_2O$ [Figure 8(*b*)] reveals that the reorganisation energy term becomes more important, and, moreover, is now greater for the trimer than for the dimer. In the former, the water moiety is reorganised about lithium from a linear O–Li–N framework to an angle of *ca.* 110° while for the latter the donor is only moved to *ca.* 127° (Figure 7). The stabilisation due to the formation of new bonds still favours the trimer and overrides the reorganisation energy deficit. Thus in the case of $H_2NLi{\cdot}H_2O$ the formation of the trimer is marginally preferred (by *ca.* 2.5 kcal mol^{-1} as opposed to *ca.* 7.8 kcal mol^{-1} earlier). However, these calculations show that in the case of bulkier solvents at Li, used in practice, the reorganisation energy term could well become dominant and so association to form the dimer would be preferred.

Reasons for the occurrence of isolated $(NLi)_n$ *rings.* A further general feature to be explained is why the $(NLi)_n$ ring systems of

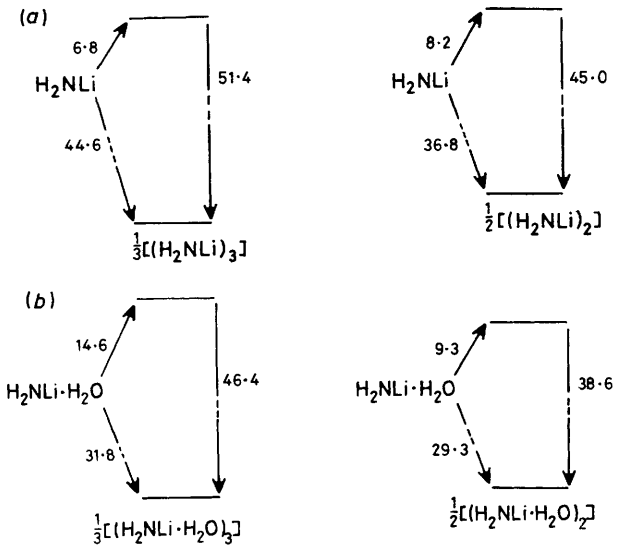

Figure 8. Calculated energy profiles (6-31G level, kcal mol^{-1}) for formation from monomeric units of (*a*) $(H_2NLi)_n$, n = 3 and 2, (*b*) $(H_2NLi{\cdot}H_2O)_n$, n = 3 and 2

(**1**), (**2**), and (**3**) do not associate further. In (**1**) particularly, the Li atoms are, most unusually, merely two-co-ordinate, so that association of such a ring might have been expected, thus relieving the co-ordinative unsaturation of the metal atoms. Indeed, apart from (**1**), $[(Me_3Si)_2NLi]_3$,[3b] and $[Me_2C(CH_2)_3CMe_2NLi]_4$,[4a] uncomplexed amidolithium compounds, $(R_2NLi)_n$, isolated so far are seemingly polymeric materials; typically being hydrocarbon-insoluble, high-m.p., amorphous powders.[12] The same is true of many iminolithium species, $(R_2C{=}NLi)_n$, which, we have argued,[6a,b] are composed of multiply stacked $(R_2C{=}NLi)_3$ trimers; although where R groups are bulky stacking is limited to two trimeric rings, so giving crystalline hexamers, $(R_2C{=}NLi)_6$. Such stacking, whether continuous or restricted, is facilitated since the R groups will lie in the $(NLi)_3$ ring plane. It will not be allowed for $(R_2NLi)_3$ systems [Figure 6(*a*)] since the R groups project above and below such a plane. For (**1**) this geometry is seen particularly well, Figure 2 illustrating why *vertical* association to a $(R_2NLi)_6$ system having three-co-ordinate Li atoms, or to even higher $(R_2NLi)_{3n}$ ones (n = 3, 4 *etc.*, with four-co-ordinate inner-ring Li atoms) is not possible. However, the steric features of $R_2C{=}N-$ and R_2N- ligands just outlined make it clear that only the latter can in principle allow *lateral* association of $(NLi)_3$ rings; N–Li edges [rather than $(NLi)_3$ faces] being joined and so giving ladder-type structures (rather than stacks). Where such association is easy sterically, the high oligomers or polymers $(R_2NLi)_{3n}$ referred to above may occur, though the ladder length can be restricted by the presence of terminal donors, as in the structure of $\{[H_2C(CH_2)_3NLi]_3{\cdot}MeN(CH_2CH_2NMe_2)_2\}_2$.[7] Once more though, Figure 2 illustrates why even this laddering option is not available for (**1**).

In complexes (**2**) and (**3**), the Li atoms are three-co-ordinate so that these dimeric rings might also have been expected to associate further, just once, producing tetramers. Such dual association occurs in the iminolithium complex $(Ph_2C{=}NLi{\cdot}NC_5H_5)_4$ which can be viewed as two stacked dimers.[6c] However, for (**2**) and (**3**) any association could not be vertical [the projection of $PhCH_2$ groups above and below the $(NLi)_2$ ring plane is clearly seen for (**2**) in Figure 4], and in these cases even lateral association is precluded, this time by the presence of the donor molecules, one on each Li atom.

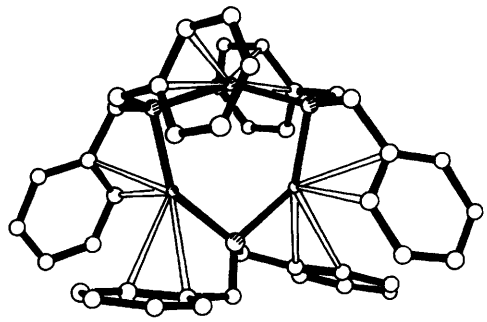

Figure 9. Lithium · · · phenyl C/CH contacts (shown as open bonds) in the crystal structure of (**1**)

The fact that the Li atoms in (**1**) are prevented sterically from association as a means of increasing their formal co-ordination number beyond two raises the question of how else co-ordinative unsaturation might be relieved. The clearest option is utilisation of the electron density potentially available from the C and H atoms, and/or from the C–H bonds, of the $PhCH_2$ units present *within* the molecule of (**1**), *i.e.* in effect to use these internal atoms or bonds as weak Lewis bases. The evidence for such intramolecular interactions is now presented.

Evidence for Intramolecular Li · · · HC *Interactions in the Solid-state Structure of* (**1**) *and in Solutions of* (**1**) *and* (**2**).—Lithium · · · HC interactions have been proposed, so far largely on the basis of relatively short Li · · · HC distances, to contribute significantly to the stereochemistry and bonding of several lithium compounds: *e.g.* $(LiC_6H_{11})_6$ (C_6H_{11} = cyclohexyl), with mean Li · · · H distances of 2.00—2.33 Å,[15] and $(LiBMe_4)_n$, with mean Li · · · H distances of 2.12—2.23 Å and mean Li · · · C of 2.21—2.36 Å.[16] Such interactions have also been proposed to influence product identities: *e.g.* in the mixed-metal cluster $LiNa_3{\cdot}(hmpa)_3{\cdot}[N{=}C(NMe_2)_2]_4$, Li · · · guanidine interactions may explain why the Li atom, unlike the Na ones, does not accommodate an hmpa molecule,[17] while second lithiations of monolithiated aromatic rings are regiospecific, possibly being directed by Li · · · *peri*–H interactions.[18] However, such proposals remain contentious, a common view being that while such interactions may be important in some specific cases, they are not a general stabilising feature in lithium chemistry. Evidence supporting such a view (with which we agree, having implied earlier that these interactions are expected most when lithium is in a formally low-co-ordinate environment) includes the observation of much longer Li · · · H distances (most >0.5 Å longer) in $[Li(SiMe_3)]_6$[19] compared to those in isostructural $(LiC_6H_{11})_6$, and PRDDO m.o. calculational results[20] on planar $(LiMe)_n$, n = 4, 5, or 6, which show small Li · · · H atomic overlap populations. However, for more realistic T_d, tetramer, and D_{3d}, hexamer, forms, analogous populations were larger despite similar Li · · · H distances, implying that Li · · · H/C distances alone are unlikely to be a good guide to the importance of these metal–hydrocarbon interactions. Nonetheless, in the structure of (**1**), there appear to be genuine interactions between Li atoms and benzyl groups, and those involving the phenyl rings are illustrated in Figure 9. Each Li atom has four contacts of <3.02 Å to methylene C atoms (average 2.81, shortest 2.69 Å), and Li(4) and Li(6) have three and two contacts respectively with methylene protons (average 2.81 and 2.71 Å respectively). In addition, each Li atom is relatively close to two α-carbon ring atoms of benzyl units on separate N atoms (average 2.80, shortest 2.60 Å), and to two *ortho*-CH units (to C, average 2.80, shortest 2.70 Å; to H, average 2.66, shortest 2.32 Å). Although

Table 9. Results of MOBI calculations on the dibenzylamidolithium compounds

Compound	Valencies		Charges		Bond indices[a]			
	Li	N	Li	N	Li–N	Li · · · Li	Li–O	Li · · · other[b]
(1)	1.44	2.70	+0.18	−0.27	0.24 × 2	0.11 × 2		0.57
					(33)	(15)		(40)
(2)	1.42	2.71	+0.20	−0.17	0.30 × 2	0.12	0.11	0.44
					(42)	(8)	(8)	(31)
(3)	1.44	2.69	+0.19	−0.16	0.28 × 2	0.11	0.19	0.45
					(39)	(8)	(13)	(32)

[a] Values in parentheses refer to the percentage contribution of the interactions to the total valency of lithium. [b] The sum of Li · · · benzyl interactions involving CH_2, and *o*-CH and α-C of the phenyl ring.

the Li · · · CH_2 distances may be necessarily quite short for a reasonable co-ordination geometry of the N atoms, the Li · · · phenyl interactions appear to represent a deliberate bending of the benzyl groups towards the Li atoms, not imposed by steric restrictions. In contrast, corresponding distances in complexes (**2**) and (**3**) all exceed 3 Å.

To probe the significance of these relatively short contacts described for (**1**), CNDO-based molecular orbital bond index (MOBI) calculations[21] were carried out using the crystal co-ordinates available for (**1**) and, to provide comparisons, for (**2**) and (**3**). Such calculations give a measure (bond indices) of the covalent bonding within a particular species. Although lithium compounds are largely ionic and quite low level calculations may be thwarted by previously noted basis set superposition errors,[22] in this instance it is reasonable to suppose that Li · · · HC interactions, involving low polarity C–H bonds, will have considerable covalent character, and that any concomitant weakening of interacting C–H bonds will be detectable through a lowering of their bond indices. The major results of these calculations are shown in Table 9. The low lithium valencies reflect the ionic nature of such species; in fact the CNDO-derived atomic charges are probably unrealistically low, and, for example, extended Hückel values imply that the charge on Li in such species is between +0.4 and +0.6. These valencies (summations of all the bond indices involving Li) are also surprisingly similar for (**1**) and for complexes (**2**) and (**3**), despite rather weaker Li–N bonding in (**1**) and the lack of Li–O (donor) bonds (the indices for which confirm the particularly good co-ordination of hmpa to Li alluded to earlier). Some compensation may come from the second Li · · · Li contact available to each Li in trimeric (**1**), although *ab initio* calculations[14,23] indicate that such cross-ring contacts in these highly ionic species may be antibonding in nature. Rather more compensation seemingly results from more, and more effective, interactions with C and H atoms in the N-attached benzyl units; although individually small, cumulatively they contribute significantly to lithium valencies (final column of Table 9). These are mirrored in consequent weakening of the C–H bonds so that, typically, an 'interacting' *ortho*-C–H bond index is *ca.* 0.89 compared to *ca.* 0.97 for an *ortho*-C–H bond distant from all the Li atoms.

Evidence from Solution Studies.—(*a*) *Electronic spectroscopy.* Solid complexes (**1**), (**2**), and (**3**) dissolve in aromatic solvents; (**1**) and (**2**) giving pink to red solutions, (**3**) deep red to purple ones. Such observations are initially perplexing since, for organolithium compounds $(LiR)_n$, colours are usually associated with charge delocalisation from the carbanionic α-C into an unsaturated ligand system, *e.g.* red when R = $PhCH_2$, green when R = naphthyl.[24] However, for dibenzylamidolithium species delocalisation from the amido $N^{\delta-}$ centre into the phenyl rings is expected to be largely blocked by the intervening methylene groups. This has been confirmed through extended Hückel calculations on $(PhCH_2)_2NH$, for which the charge on N is 0.64 e, and on its amide ion, $(PhCH_2)_2N^-$, for which the charge on N is 1.40 e; *i.e.* most of the excess charge (*ca.* 0.8 e) remains on the N atom. Accordingly, the origins of the solution colours of (**1**), (**2**), and (**3**) were investigated as follows. The u.v.–visible spectra (800—280 nm) of benzene solutions of (**1**), (**2**), and (**3**) of known concentrations were recorded under nitrogen in sealed glass cells. Details of major absorbance bands in or near the visible region are presented in Table 10, from which it is seen that solutions of (**1**) and (**2**) both showed a similar band in the visible spectrum (at *ca.* $\lambda_{max.}$ 525 nm) of fairly weak absorptivity. However, the relative intensities of these bands increased on dilution, *e.g.* for (**1**), a ten-fold dilution gave a three-fold increase in absorptivity. These results imply, therefore, that the colours of solutions of (**1**) and (**2**) are due to a 'forbidden' charge-transfer species common to both (thus, a non-ether co-ordinated species) and presumably one of low association. The hmpa complex (**3**) gives very different electronic spectra, with the colour of its solutions being due to a much more intense band (at 565 nm) whose absorptivity decreases slightly on dilution. In addition, in the spectrum of the more concentrated solution, a second strong band is apparent (at *ca.* 320 nm), though this decreases dramatically in absorptivity on dilution. It seems likely that the colour-giving band arises from 'allowed' charge transfer, presumably within a solution species that retains hmpa co-ordinated to Li. The absorption at lower wavelength may represent a close-contact (tight ion pair) solution species, $(PhCH_2)_2N^-,Li^+$·hmpa, which on dilution partially dissociates to a looser (solvent-separated ion pair) arrangement, $(PhCH_2)_2N^-$ · · · $Li^+(hmpa)_x$.

Table 10. Experimental u.v.–visible absorptions ($\lambda_{max.}$) for benzene solutions of the dibenzylamidolithium compounds

Compound	Concentration/ mol dm^{-3} *	$\lambda_{max.}$/ nm	Absorptivity/ dm^3 mol^{-1} cm^{-1}
(1)	5.3×10^{-3}	525	100
	5.3×10^{-4}	530	295
(2)	9.8×10^{-3}	520	40
	4.9×10^{-4}	525	65
(3)	1.2×10^{-3}	565	2 100
		(315)	(1 645)
	5.8×10^{-4}	565	1 600
		(320)	(260)

* With respect to empirical formulae, *i.e.* monomeric species.

(*b*) *Relative molecular mass* (*r.m.m.*) *cryoscopic measurements and* ^{7}Li *n.m.r. spectroscopy.* The results for solutions of (**1**) and (**2**) have been alluded to in a paper concerned with the applications of these two techniques to the study of lithium compounds in general.[8] Briefly, r.m.m. values for benzene

solutions of (1) decreased on dilution, giving average association states (n) of 2.87 (3.3×10^{-2} mol dm^{-3}) to 2.66 (2.5×10^{-2} mol dm^{-3}). Such values imply that, while the trimer largely persists, dimeric and/or monomeric species are also present. In contrast, n values for solutions of (2) are much less than 2, varying between 1.20 (3.1×10^{-2} mol dm^{-3}) and 1.07 (1.8×10^{-2} mol dm^{-3}) and so point either to extensive dissociation of the diethyl ether co-ordinated dimer into an ether co-ordinated monomer, or to loss of ether to give $[(PhCH_2)_2NLi]_n$ species, which presumably would engage in trimer $\rightleftharpoons$ dimer/monomer equilibria similar to those noted for (1). The latter is far more likely, given the lability of the diethyl ether in solid (2) on heating, and the common $\lambda_{max.}$ absorption band found for solutions of (1) and (2). Once more, (3) behaves very differently, giving essentially constant n values of 1.34 and 1.36 over varying concentrations (3.1×10^{-2} and 1.9×10^{-2} mol dm^{-3} respectively).

The ^{7}Li n.m.r. spectra of [$^2H_6$]benzene solutions of (1) and (2) are, like their electronic spectra, extremely similar. In relatively concentrated solutions (1.7×10^{-1}—2.6×10^{-1} mol dm^{-3}) a single resonance, essentially coincident, is observed for (1) (at δ −0.66 p.p.m.) and for (2) (at δ −0.65 p.p.m.). Hence, for the latter, essentially complete dissociation of ether is implied even at these quite high concentrations (note that, to permit reasonable acquisition times, solutions used for n.m.r. spectroscopy are much more concentrated than those for electronic spectroscopy or cryoscopy), the uncomplexed $[(PhCH_2)_2NLi]_n$, formally with $n = 2$, rearranging to give the trimer ($n = 3$) as found in (1). On dilution to *ca.* 5.0×10^{-2} mol dm^{-3}, the ^{7}Li n.m.r. spectra of (1) and (2) again show this common resonance attributable to $[(PhCH_2)_2NLi]_3$, but second, less intense signals appear at the same, now very low, frequency (δ −2.91 p.p.m.) for both compounds. Taken along with the earlier electronic spectroscopic and cryoscopic results, these signals can be assigned with confidence to $[(PhCH_2)_2NLi]_n$, with $n = 1$ or 2, such species being responsible for solution colours. Characteristically, solutions of (3) have entirely different ^{7}Li n.m.r. spectra, those acquired for relatively concentrated solutions already having two signals at δ −0.31 and δ −1.53 p.p.m., relative intensities *ca.* 50:1 (*cf.* the two absorptions observed at 565 and 320 nm in the u.v.–visible spectrum). On dilution, the more intense signal is retained (δ −0.30 p.p.m.), the less intense one being replaced by a new resonance at δ −1.30 p.p.m. (relative intensities *ca.* 25:1); *cf.* the drastic diminution of the electronic absorption band at 320 nm, but the essential retention of that at 565 nm, on dilution. Although an explanation of such data must be speculative, the electronic and n.m.r. spectroscopic results correlate qualitatively and it seems likely that the 565 nm, δ −0.30 p.p.m. absorptions are due to molecular $[(PhCH_2)_2NLi{\cdot}hmpa]_2$; the non-observation of a resonance at *ca.* δ −0.65 p.p.m. makes it clear that hmpa does not dissociate when solid (3) is dissolved, so that $[(PhCH_2)_2NLi]_n$ species are not formed. Given the r.m.m. results, showing n *ca.* 1.3, some dissociation occurs, but it must be to a monomer $(PhCH_2)_2NLi{\cdot}hmpa$ which, in relatively concentrated solution, might be a tight ion pair (giving absorptions at 320 nm, δ −1.53 p.p.m.) though becoming looser on dilution (hence these absorptions diminish or disappear, and, in the n.m.r. spectrum, a new resonance appears at δ −1.30 p.p.m.).

(*c*) *Molecular orbital calculations.* The above results implied that, for (1) and (2), an uncomplexed species, $[(PhCH_2)_2NLi]_n$, with $n = 1$ or 2, is responsible for the unusual solution colours observed. Furthermore, such a species might, given the solid-state data observed for (1), be expected to exhibit enhanced Li···HC interactions. To explore these implications, the excited states of (1) and (2), and of fragments taken from them by using selected atomic co-ordinates from crystal structure data, were calculated by a configuration interaction method which has proved successful in predicting the electronic spectra of main group compounds.[25] For the larger species, some idealisations of the molecules were required and details of these and of the predicted highest wavelength (h.o.m.o.→l.u.m.o., highest occupied and lowest unoccupied molecular orbital) transitions for all species are given in Table 11. The key feature is that the only visible region $\lambda_{max.}$ absorptions predicted to occur are those for uncomplexed monomeric dibenzylamidolithium; the $\lambda_{max.}$ value for this species derived from the co-ordinates of (2) in particular agreeing well with the experimental value of *ca.* 520 nm. Complexation of the monomer by diethyl ether, or association to a dimer (with and without a donor) or to a trimer, all result in striking shifts into the u.v. region. The same applies for other conceivable solution species such as dibenzylamide ion [though the value here is very similar to that at *ca.* 320 nm found in solutions of (3) and attributed earlier to ion pairs involving $(PhCH_2)_2N^-$ and $Li^+{\cdot}$hmpa]. The value of $\lambda_{max.}$ for dibenzylamine, which would be produced on slight hydrolysis of the amidolithium solutions, was calculated in order to gauge the confidence which could be placed in this m.o. method; pleasingly, the values in Table 11 agree well with the experimental $\lambda_{max.}$ in cyclohexane solution of 277 nm.

Table 11. Predicted absorptions ($\lambda_{max.}$) for (1) and (2), and for fragments of them

Species	Deriv-ation[a]	Association state	Predicted $\lambda_{max.}$/nm
$[(PhCH_2)_2NLi]_2[H_2NLi]$	(1)	Trimer	255
$[(PhCH_2)_2NLi{\cdot}OH_2]_2$	(2)	Complexed dimer	294
$[(PhCH_2)_2NLi]_2$	(2)	Dimer	320
$(PhCH_2)_2NLi{\cdot}OEt_2$	(2)	Complexed monomer	396
$(PhCH_2)_2NLi$	(1)	Monomer	685—461[b]
	(2)	Monomer	546
$(PhCH_2)_2N^-$	(1)		323
$(PhCH_2)_2NH$	(1)		285
	(2)		290

[a] Co-ordinates for the calculations were taken from crystal structure co-ordinates, with appropriate adjustments where some idealisation of the molecule was necessary. [b] Values vary between these limits depending on which of the three fragments of (1) is considered.

Concerning such a hydrolysis product, since the initial communication of this work[5] we have considered one further possible explanation of the solution colours observed for (1) and (2), namely that their slight hydrolysis produces dibenzylamine which then complexes to some of the dibenzylamidolithium present, giving a coloured species. Such a process would presumably be encouraged on dilution, and so might explain the increasing electronic absorbance at *ca.* 520 nm and the growth of the ^{7}Li n.m.r. resonance at δ −2.90 p.p.m. To investigate this possibility, we have isolated such a complex *via* the reaction of n-butyl-lithium in hexane with two molar equivalents of dibenzylamine. Cooling of the resulting solution produced very deep red crystals of $[(PhCH_2)_2NLi{\cdot}HN(CH_2Ph)_2]_n$, m.p. 48—50 °C. [In the solid state, this complex is dimeric ($n = 2$) with an $(N_{amido}Li)_2$ central ring and each Li having a terminally attached amine ligand.][26] However, the solution spectra of this compound do not correlate with those of solutions of (1) and (2). For example, in the ^{7}Li n.m.r. spectra of [$^2H_6$]benzene solutions of varying concentrations at 25 °C, broad resonances at δ −0.09 to −0.36 p.p.m. are observed, but there is no signal at *ca.* δ −2.9 p.p.m. Such a signal (at δ −2.87 p.p.m.), though small relative to major ones at −0.16 to −0.25, is apparent in

Table 12. Crystal data and structure determination

	(1)	(2)	(3)
Formula	$C_{42}H_{42}Li_3N_3$	$C_{36}H_{48}Li_2N_2O_2$	$C_{40}H_{64}Li_2N_8O_2P_2$
M	609.6	554.7	764.8
Crystal system	Triclinic	Monoclinic	Monoclinic
Space group	$P\bar{1}$	$C2/c$	$P2_1/n$
a/Å	10.191(1)	23.842(5)	10.699(2)
b/Å	12.511(1)	10.806(2)	20.611(2)
c/Å	15.444(2)	14.841(3)	11.587(2)
α/°	73.98(1)		
β/°	76.59(1)	116.64(1)	115.18(1)
γ/°	72.22(1)		
U/Å^3	1 778.6	3 417.7	2 312.3
Z	2	4	2
D_c/g cm^{-3}	1.138	1.078	1.098
$F(000)$	648	1 200	824
μ(Mo-K_α)/mm^{-1}	0.06	0.06	0.13
Crystal size/mm	0.17 × 0.42 × 0.70	0.40 × 0.40 × 0.45	0.25 × 0.35 × 0.50
Crystal colour	Pale pink	Pale pink	Purple-red
No. of reflections for cell	32	33	22
2θ Range for cell/°	20—25	20—25	20—25
$2\theta_{max.}$ for data collection	45	45	45
Reflections measured	4 633	3 686	5 067
Unique reflections	4 633	2 221	3 019
Reflections with $F > n\sigma(F)$	3 063	1 469	1 939
n	4	4	3
R_{int}		0.071 (2θ > 35° only)	0.028
g in weighting formula	0.001 05	0.000 40	0.002 07
No. parameters	433	197	244
R	0.058	0.078	0.096
$R' = (\Sigma w\Delta^2/\Sigma wF_o^2)^{\frac{1}{2}}$	0.066	0.066	0.109
Max. and mean shift/e.s.d.	0.015, 0.004	0.113, 0.020	0.016, 0.005
Slope of normal probability plot	1.23	1.29	1.25
Max., min. features in final difference map/e Å^{-3}	+0.17, −0.27	+0.18, −0.21	+0.33, −0.38

the spectra of [$^2H_8$]toluene solutions, particularly dilute ones. This, however, is not surprising (though it does imply a solvent effect) as dissociation of amine ligand from the complex on dissolution (n values by cryoscopy in benzene range from 1.20 to 0.95 for 9.7 × 10^{-2}—2.2 × 10^{-2} mol dm^{-3} concentrations respectively) would presumably allow precisely the same solution equilibria noted earlier for (**1**) and (**2**). It seems clear then that this amine complex is not responsible for the latters' observed solution colours, though its formation due to slight surface hydrolysis may explain the pale pink colours of isolated crystals of (**1**) and (**2**).

Though relating strictly to vapour phase species, the above predictive m.o. calculations do seem, when judged in concert with experimental spectroscopic and cryoscopic data, to confirm that monomeric dibenzylamidolithium, $(PhCH_2)_2NLi$, is indeed responsible for the observed solution colours of (**1**) and (**2**). The same calculations show that within such a species, whether derived from the co-ordinates of (**1**) or (**2**), the h.o.m.o. is a combination of ligand backbone atomic orbitals provided by the N atom, the CH_2 atoms of the methylene groups, the α-C atoms of both of the phenyl rings, and one set of the o-CH atoms on each of these rings, *i.e.* precisely the same combination of atoms involved in the supposed Li • • • HC interactions within solid trimeric (**1**). The l.u.m.o. is made up of Li atomic orbitals, so clearly the colour-giving transition is of the charge transfer type. The implication is that Li • • • benzyl interactions, present in the solid trimer whose Li atoms are two-co-ordinate, become much larger in solution within a monomeric species whose Li atom is merely one-co-ordinate. In turn, this increased involvement of the benzyl (h.o.m.o.) and Li (l.u.m.o.) units allows the charge transfer mechanism to operate, thereby producing the h.o.m.o.→l.u.m.o. bathochromic shift into the visible region (*cf.* $\lambda_{max.}$ values predicted for trimeric and monomeric dibenzylamidolithium in Table 11). Further support for this contention comes from MOBI calculations on such a monomer, using just one-third of the co-ordinates available for solid (**1**). Comparing the results with those noted earlier for (**1**) in its entirety (see Table 9), the Li valency understandably falls to 1.13 but this is largely due to the loss of a second Li–N bond since summed Li • • • HC indices (Li • • • other in Table 9) remain essentially the same, at 0.51, and thereby contribute a greater percentage (45%) to the overall Li valency. It follows, of course, that since the Li atom in the monomer has far fewer Li • • • HC contacts than it did when part of the trimer, individual Li • • • H and Li • • • C indices increase markedly, and that they do so despite the assumption of precisely the same Li • • • H and Li • • • C distances. Although the detailed solution structure of monomeric $(PhCH_2)_2NLi$ is obviously unknown, the implication is that here the $PhCH_2$ groups are much closer to the Li.

Experimental

Standard inert-atmosphere techniques were used for the preparations and characterisations of compounds (**1**), (**2**), and (**3**). Analytical values (C, H, and N determined using a Perkin-Elmer 240 elemental analyser, Li on a 360 Perkin-Elmer atomic absorption spectrometer, and [for (**3**)] P by gravimetric analysis *via* precipitation of a phospho-molybdate complex) are recorded in Table 1 along with a description of the compounds, the yields obtained, and their melting points.

Synthesis of $[(PhCH_2)_2NLi]_3$ (**1**).—A hexane solution of n-butyl-lithium (2.7 cm^3 of a 1.84 mol dm^{-3} solution, 5.0 mmol) was added to a chilled solution of dibenzylamine (0.99 g, 5.0 mmol) in toluene–hexane (2:1, 15 cm^3). A very pale pink solid within a red solution was produced immediately. Warming to 60 °C and slow addition of more toluene (10 cm^3) effected complete dissolution, cooling of the resulting solution giving pale pink crystals which were washed with hexane, dried, and identified as (**1**).

Synthesis of $[(PhCH_2)_2NLi{\cdot}OEt_2]_2$ (**2**).—Treatment of a chilled solution of dibenzylamine (1.97 g, 10.0 mmol) in diethyl ether–hexane (3:2, 25 cm^3) with n-butyl-lithium (7.1 cm^3 of a 1.41 mol dm^{-3} solution in hexane, 10.0 mmol) resulted in the formation of a red solution and a white or pale pink crystalline precipitate. Warming of this mixture to 35 °C caused complete dissolution, subsequent slow cooling providing very pale pink crystals of (**2**).

Synthesis of $[(PhCH_2)_2NLi{\cdot}hmpa]_2$ (**3**).—n-Butyl-lithium (3.2 cm^3 of a 1.56 mol dm^{-3} solution in hexane, 5.0 mmol) was added slowly to a stirred and cooled solution of dibenzylamine (0.99 g, 5.0 mmol) and hmpa (0.90 g, 5.0 mmol) in hexane (10 cm^3). A deep red solid was obtained almost immediately, though this dissolved on warming to 60 °C. Cooling gave large purple crystals of (**3**).

The spectroscopic data were obtained as follows. The ^7Li n.m.r. spectra were recorded on a Bruker WH 360-MHz n.m.r. spectrometer operating for ^7Li at 139.19 MHz, [$^2H_6$]benzene or [$^2H_8$]toluene solutions being externally referenced to the ^7Li signal of phenyl-lithium in the same solvents (Ξ values, 38.863 883 and 38.863 882 MHz respectively). For u.v.–visible spectroscopic studies, benzene solutions of (**1**), (**2**), and (**3**) of known concentrations were prepared in graduated flasks inside a glove-box, then placed in sealed 1-cm glass cells prior to recording the spectra on a Beckmann spectrophotometer ACTA MIV instrument. Cryoscopic r.m.m. measurements on variable-concentration benzene solutions of (**1**), (**2**), and (**3**) were carried out as previously described.[8]

Molecular orbital bond index (MOBI) calculations were run within a modified CNDO-MO-SCF framework, program MOSC 170, on an ICL 2900 computer, and in selected cases by SCF followed by configuration interaction methods using a suite of programs on ICL 19045 hardware; all software by Professor P. G. Perkins. The optimised geometries described were obtained from the *ab initio* computer program GAMESS[27] using the 6-31G basis set.[28]

Crystals of compounds (**1**), (**2**), and (**3**) suitable for *X*-ray analysis were transferred in a nitrogen-filled glove box to glass Lindemann capillary tubes which were then sealed prior to data collection. All *X*-ray diffraction computer programs used in this study were written by W. C. and Professor G. M. Sheldrick. Calculations were performed on a Data General Eclipse S/250 computer.

X-*Ray Crystallography*.—Crystal data and information concerning structure determination are given in Table 12. Data were collected at room temperature on a Stoe-Siemens AED diffractometer with graphite-monochromated Mo-K_α radiation (λ = 0.710 69 Å); intensity measurements employed ω–θ scans and an on-line profile fitting technique.[29] Cell parameters were refined from 2θ values of reflections centred at ±ω. No absorption or extinction corrections were applied. Atomic scattering factors were taken from ref. 30. The structures were solved by direct methods, and refined on *F* by blocked-cascade least squares with the weighting scheme $w^{-1} = \sigma^2(F) + gF^2$.[31]

Additional material available from the Cambridge Crystallographic Data Centre comprises: thermal parameters, H-atom co-ordinates, and remaining bond lengths and angles.

Acknowledgements

We thank the S.E.R.C. (D. B., R. E. M., and R. S.), the Royal Society (Research Fellowship to R. E. M.), and the Verband der Chemischen Industrie (W. C. at the University of Göttingen) for financial support, the S.E.R.C. for provision of high-field n.m.r. facilities, Professor P. G. Perkins for the use of his m.o. calculation programs, and Professor K. Wade for many useful discussions.

References

1 M. F. Lappert, P. P. Power, A. R. Sanger, and R. C. Srivastava, 'Metal and Metalloid Amides,' Ellis Horwood-Wiley, Chichester, 1980.
2 (*a*) J. C. Stowell, 'Carbanions in Organic Synthesis,' Wiley-Interscience, New York, 1979; (*b*) M. Fieser, 'Fieser's Reagents for Organic Synthesis,' Wiley-Interscience, New York, 1986, vol. 12 and earlier volumes.
3 (*a*) D. C. Bradley and R. G. Copperthwaite, *Inorg. Synth.*, 1978, **18**, 112; (*b*) R. D. Rogers, J. L. Atwood, and R. Grüning, *J. Organomet. Chem.*, 1978, **157**, 229.
4 (*a*) M. F. Lappert, M. J. Slade, A. Singh, J. L. Atwood, R. D. Rogers, and R. Shakir, *J. Am. Chem. Soc.*, 1983, **105**, 302; (*b*) L. M. Engelhardt, A. S. May, C. L. Raston, and A. H. White, *J. Chem. Soc., Dalton Trans.*, 1983, 1671.
5 D. Barr, W. Clegg, R. E. Mulvey, and R. Snaith, *J. Chem. Soc., Chem. Commun.*, 1984, 285, 287.
6 (*a*) D. Barr, W. Clegg, R. E. Mulvey, R. Snaith, and K. Wade, *J. Chem. Soc., Chem. Commun.*, 1986, 295; (*b*) D. R. Armstrong, D. Barr, R. Snaith, W. Clegg, R. E. Mulvey, K. Wade, and D. Reed, *J. Chem. Soc., Dalton Trans.*, 1987, 1071; (*c*) D. Barr, R. Snaith, W. Clegg, R. E. Mulvey, and K. Wade, *ibid.*, p. 2141.
7 D. R. Armstrong, D. Barr, W. Clegg, R. E. Mulvey, D. Reed, R. Snaith, and K. Wade, *J. Chem. Soc., Chem. Commun.*, 1986, 869.
8 D. Reed, D. Barr, R. E. Mulvey, and R. Snaith, *J. Chem. Soc., Dalton Trans.*, 1986, 557.
9 A-M. Sapse, E. Kaufmann, P. v. R. Schleyer, and R. Gleiter, *Inorg. Chem.*, 1984, **23**, 1569.
10 B. Çetinkaya, P. B. Hitchcock, M. F. Lappert, M. C. Misra, and A. J. Thorne, *J. Chem. Soc., Chem. Commun.*, 1984, 148.
11 T. Fjeldberg, P. B. Hitchcock, M. F. Lappert, and A. J. Thorne, *J. Chem. Soc., Chem. Commun.*, 1984, 822.
12 D. Barr, W. Clegg, R. E. Mulvey, R. Snaith, and D. S. Wright, *J. Chem. Soc., Chem. Commun.*, 1987, 716.
13 D. Barr, W. Clegg, R. E. Mulvey, D. Reed, and R. Snaith, *Angew. Chem., Int. Ed. Engl.*, 1985, **24**, 328.
14 (*a*) E. U. Würthwein, K. D. Sen, J. A. Pople, and P. v. R. Schleyer, *Inorg. Chem.*, 1983, **22**, 496; (*b*) D. R. Armstrong, P. G. Perkins, and G. T. Walker, *J. Mol. Struct. (Theochem.)*, 1985, **122**, 189.
15 R. Zerger, W. Rhine, and G. Stucky, *J. Am. Chem. Soc.*, 1974, **96**, 6048.
16 W. Rhine, G. D. Stucky, and S. W. Patterson, *J. Am. Chem. Soc.*, 1975, **97**, 6401.
17 W. Clegg, R. E. Mulvey, R. Snaith, G. E. Toogood, and K. Wade, *J. Chem. Soc., Chem. Commun.*, 1986, 1740.
18 U. Schubert, W. Neugebauer, and P. v. R. Schleyer, *J. Chem. Soc., Chem. Commun.*, 1982, 1184; W. Neugebauer, A. J. Kos, and P. v. R. Schleyer, *J. Organomet. Chem.*, 1982, **228**, 107; W. Neugebauer, T. Clark, and P. v. R. Schleyer, *Chem. Ber.*, 1983, **116**, 3283.
19 W. H. Ilsley, T. F. Schaaf, M. D. Glick, and J. P. Oliver, *J. Am. Chem. Soc.*, 1980, **102**, 3769.
20 G. Graham, S. Richtsmeier, and D. A. Dixon, *J. Am. Chem. Soc.*, 1980, **102**, 5759.
21 D. R. Armstrong, P. G. Perkins, and J. J. P. Stewart, *J. Chem. Soc., Dalton Trans.*, 1973, 838, 2273; see also T. N. Bell, K. A. Perkins, and P. G. Perkins, *J. Chem. Soc., Faraday Trans. 1*, 1981, 1779; R. E. Mulvey, M. E. O'Neill, K. Wade, and R. Snaith, *Polyhedron*, 1986, **5**, 1437.
22 S. M. Bachrach and A. Streitwieser, *J. Am. Chem. Soc.*, 1984, **106**, 2283, 5818; K. C. Waterman and A. Streitwieser, *ibid.*, p. 3138.
23 D. R. Armstrong and G. T. Walker, *J. Mol. Struct. (Theochem.)*, 1986, **137**, 235; A. M. Sapse, E. Kaufmann, P. v. R. Schleyer, and R. Gleiter, *Inorg. Chem.*, 1984, **23**, 1569.
24 J. M. Mallan and R. L. Bebb, *Chem. Rev.*, 1969, **69**, 693; M. A. Fox, *ibid.*, 1979, **79**, 253.

25 D. R. Armstrong, P. G. Perkins, and J. J. P. Stewart, *J. Chem. Soc., Dalton Trans.*, 1973, 2277.
26 D. Barr, W. Clegg, R. E. Mulvey, and R. Snaith, unpublished work.
27 M. Dupuis, D. Spangler, and J. J. Wendoloski, 'GAMESS,' National Research Council Computing Software Catalogue, vol. 1, Program No. 2 GO1, 1980; M. F. Guest, J. Kendrick, and S. A. Pope, GAMESS Documentation, Daresbury Laboratory, 1983.
28 W. J. Hehre, R. Ditchfield, and J. A. Pople, *J. Chem. Phys.*, 1972, **56**, 2257; P. C. Hariharan and J. A. Pople, *Theor. Chim. Acta*, 1973, **28**, 213; J. D. Dill and J. A. Pople, *J. Chem. Phys.*, 1975, **62**, 2921.
29 W. Clegg, *Acta Crystallogr., Sect. A*, 1981, **37**, 22.
30 'International Tables for *X*-Ray Crystallography,' Kynoch Press, Birmingham, 1974, vol. 4, pp. 99, 149.
31 G. M. Sheldrick, SHELXTL, an integrated system for solving, refining, and displaying crystal structures from diffraction data, University of Göttingen, 1978.

Received 17*th February* 1987; *Paper* 7/292